Supplementary Information

Manipulating Oxidation of Silicon with Fresh Surface Enabling Stable Battery Anode

Gaofeng Ge,[†‖] Guocheng Li,[†‖] Xiancheng Wang,[†] Xiaoxue Chen,[†] Lin Fu,[†] Xiaoxiao Liu,[†] Eryang Mao,[†] Jing Liu,[†] Xuelin Yang,[‡] Chenxi Qian,[§] Yongming Sun [†*]

† *Wuhan National Laboratory for Optoelectronics, Huazhong University of Science and Technology, Wuhan 430074, China*

‡ *College of Electrical Engineering and New Energy, China Three Gorges University, 8 Daxue Road, Yichang, Hubei 443002, China*

§ *Division of Chemistry and Chemical Engineering, California Institute of Technology, 1200 E California Boulevard, Pasadena, California 91125, United States*

‖ *These authors contributed equally to this work*

* Email: *yongmingsun@hust.edu.cn* .

Methods

Fabrication of the SiO_x/C composite. Silicon dust from the solar photovoltaic industry was used as the raw material to prepare the SiO_x/C composite. The silicon waste was first ball milled for 20 h at 350 r min^{-1}. The obtained initial Si particles were then immersed in diluted hydrofluoric acid for 20 h under stirring to remove the native oxidization layer on the surface. After washing, Si particles with fresh surface were dispersed in glucose solution with Si/glucose ratio of 1:1 by weight under stirring. The mixture was then sealed in a reactor and treated at 200 °C for 20 h. The product after

hydrothermal treatment was then washed by deionized water and dried at 80 °C. The SiO_x/C composite was finally obtained after annealing of the the above precursor at 700 °C for 2 h in an Ar atmosphere.

Material Characterization. XRD results were collected by a PANalytical B.V. instrument (Empyrean) with Cu Kα radiation. TGA measurement was conducted on a TA-Q50 instrument from 30 to 800°C with a heating rate of 10°C min^{-1} in a flow air. XPS spectra were obtained on a VG MultiLab 2000 system (Thermo VG Scientific) with monochromatic Al Kα X-ray source. The morphology and microstructure of the materials were characterized by SEM (ZEISS GeminiSEM 300) and TEM (Talos F200X).

Electrochemical Measurements. Slurries for SiO_x/C electrode and graphite-SiO_x/C hybrid electrode were prepared by uniformly mixing active materials, super P carbon and sodium carboxymethyl cellulose (7:2:1 by weight for SiO_x/C electrode and 8:1:1 by weight for graphite-SiO_x/C hybrid electrode) in water, respectively. Before the fabrication of graphite-SiO_x/C hybrid electrode, SiO_x/C composite and graphite are uniformly mixed with a weight ratio of 15:85 in an agate mortar to form graphite-SiO_x/C hybrid. After The slurries were casted on a Cu foil, and then were dried at 80 °C in vacuum for 2 h. The as-fabricated electrodes were then calendered and cut into circular disks with a diameter of 10 mm. All the electrochemical measurements of the working electrodes were carried out using standard 2032-type coin cells assembled in an Ar-filled glovebox with Li foil as the counter/reference electrode, microporous polyethylene as the separator and 1 M $LiPF_6$ in ethylene carbonate/diethylene carbonate (1:1 v/v) with 2 vol% fluoroethylene carbonate additive as the electrolyte. Half cells for SiO_x/C electrode were evaluated from 0.01 V to 1 V (*vs*. Li^+/Li) at the current density of 0.05 A g^{-1} for the initial two cycles and 0.5 A g^{-1} for the subsequent cycles on Neware test system at room temperature. Figure 3(a) shows the cycling performance of the electrode with mass loading of ~0.9 mg cm^{-2}. Figure 3(c) displays the rate capability of the electrode with mass loading of ~0.4 mg cm^{-2}. Half cells for graphite-SiO_x/C hybrid electrode were evaluated from 0.01 V to 1.5 V (*vs*. Li^+/Li) at the current density of 0.02

A g^{-1} for the initial two cycles and 0.08 A g^{-1} for the subsequent cycles. The cyclic voltammetry (CV) and electrochemical impedance spectroscopy (EIS) measurements were performed on a Biologic VMP3 electrochemical workstation.

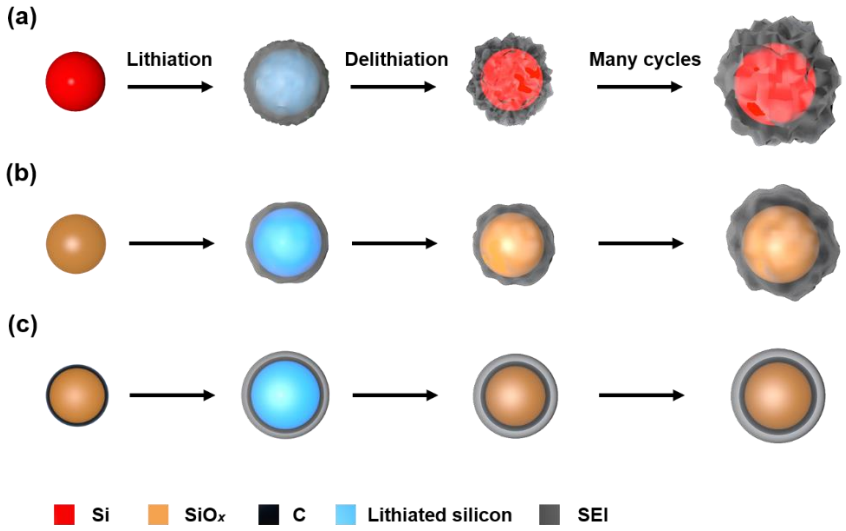

Figure S1. Schematic of electrochemical lithiation/delithiation cycling of (a) Si NPs (b) SiO_x and (c) SiO_x/C composite.

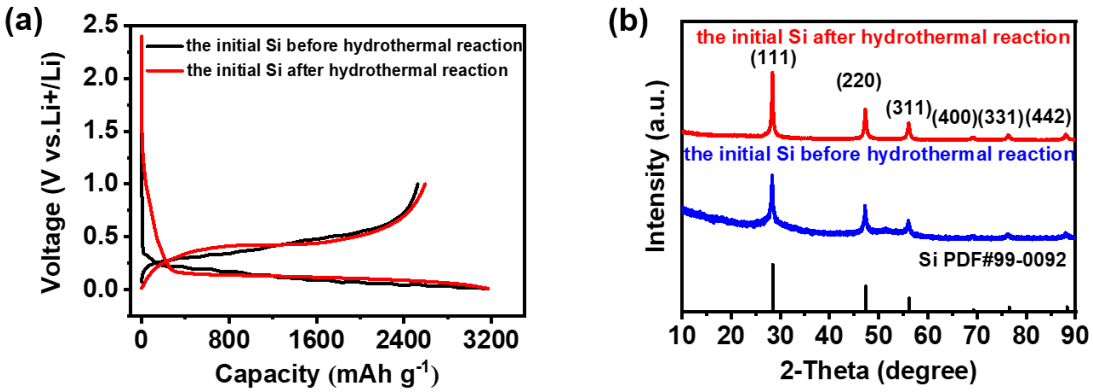

Figure S2. (a) The first specific capacity-voltage curve and (b) XRD of the initial Si particles before and after hydrothermal reaction.

After hydrothermal treatment, the first specific capacity hardly changed, indicating initial Si particles can not be oxidized under hydrothermal condition. Simultaneously, characteristic peak of silicon oxidation was not observed in the XRD pattern, which confirmed the accuracy of this view once again.

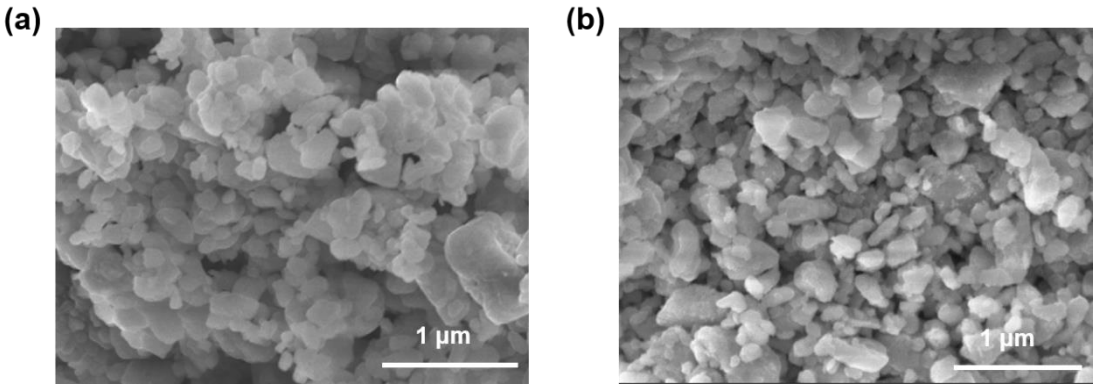

Figure S3. SEM images of the Si particles (a) before and (b) after the removal of the passivation layer.

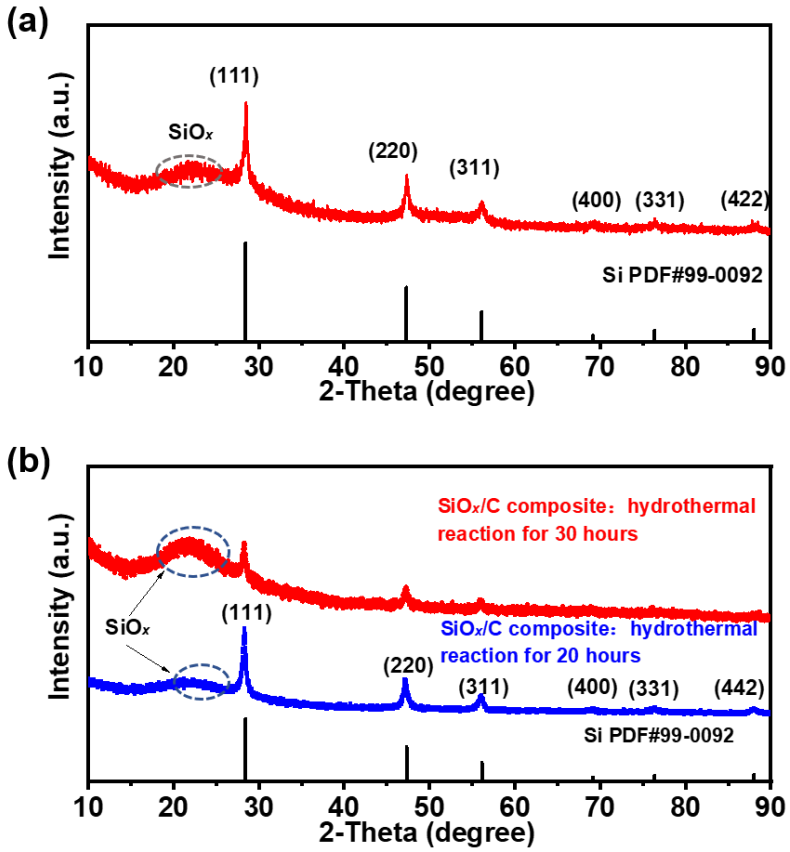

Figure S4. (a) XRD of the pristine Si particles with fresh surface after their treatment in hydrothermal and annealing treatment in Ar. (b) XRD of the as-fabricated SiO_x/C composite achieved by hydrothermal treatment for different times.

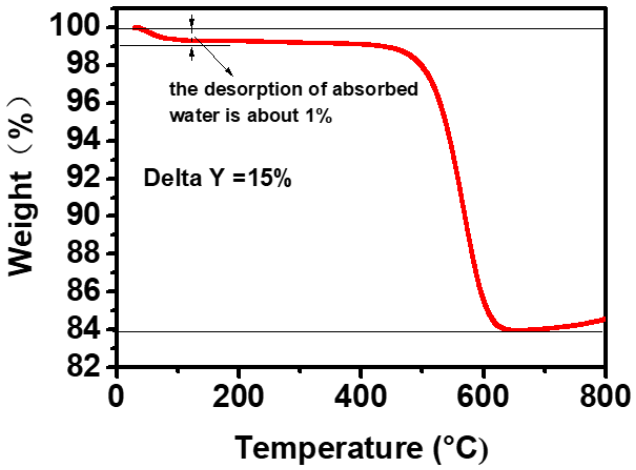

Figure S5. TGA curve of the SiO_x/C composite under air. The carbon content in the SiO_x/C composite is calculated as 15 wt%. The mass loss from room temperature to 100 ºC comes from the desorption of absorbed water. The weight loss below 650 ºC came from carbon loss. The weight started to increase after 650 ºC, which should arise from the oxidation of Si remnant.

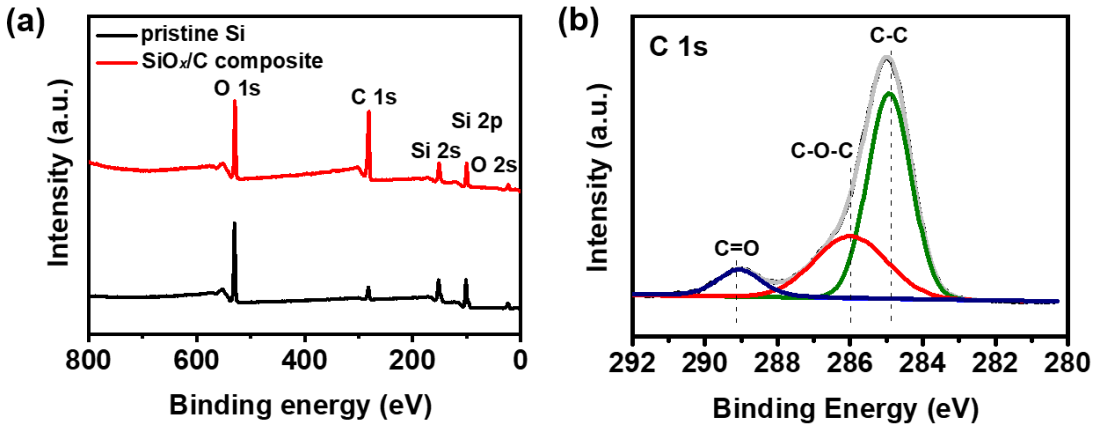

Figure S6. (a) XPS full spectra of the pristine Si and the SiO_x/C composite. (b) High-resolution XPS spectra of C 1s for the SiO_x/C composite.

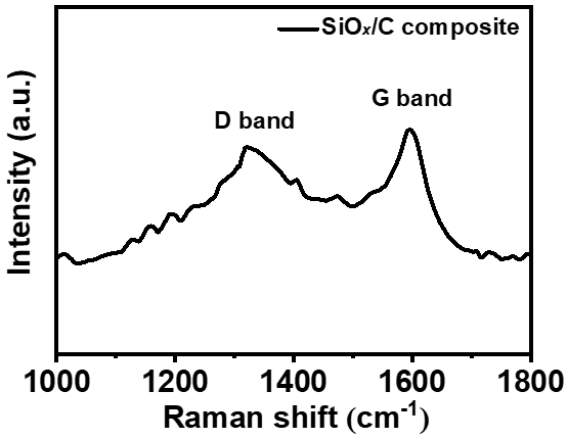

Figure S7. Raman spectra for the SiO_x/C composite. The Raman spectrum shows two broad peaks at ~1322 cm^{-1} and ~1598 cm^{-1} (corresponding to D-band and G-band of carbon, respectively), suggesting the amorphous structure of carbon in the SiO_x/C nanocomposite.

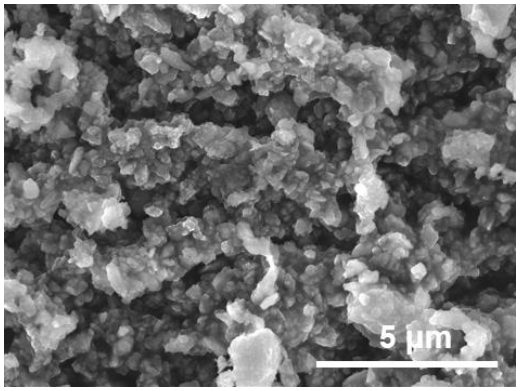

Figure S8. SEM image of the SiO_x/C composite.

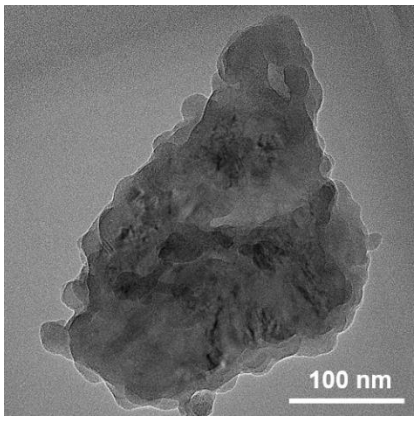

Figure S9. TEM image of the SiO_x/C composite.

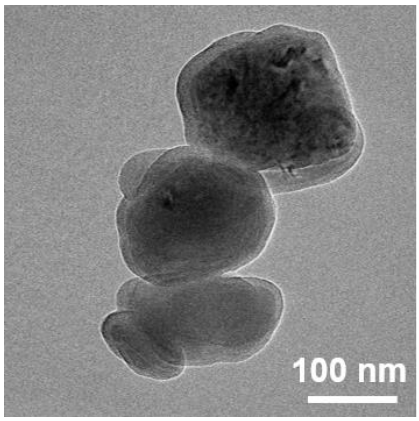

Figure S10. TEM image of pristine Si.

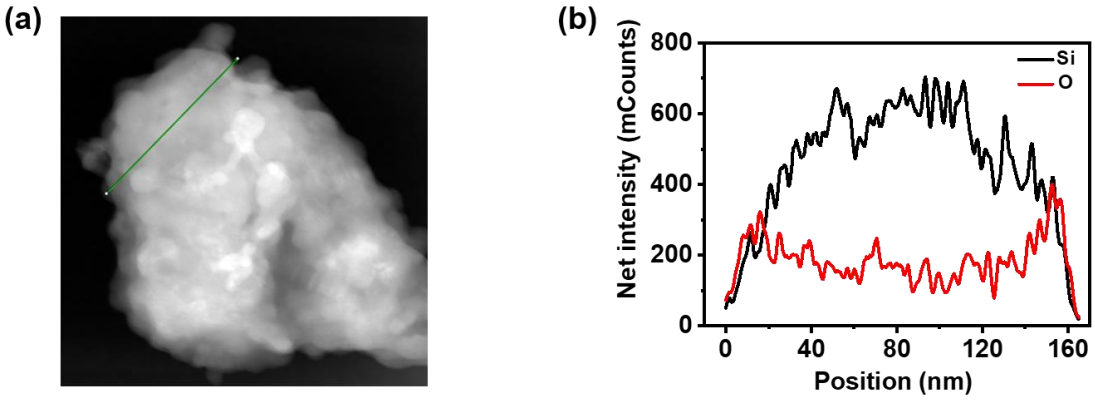

Figure S11. (a) HAADF-STEM image and (b) the corresponding EDX line scan result of a SiO_x/C composite.

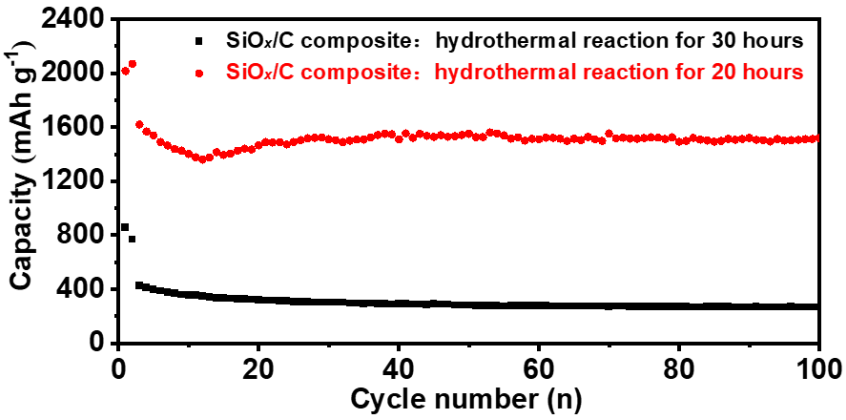

Figure S12. Capacity-cycle number plots of the SiO_x/C composite with different oxidation degrees.

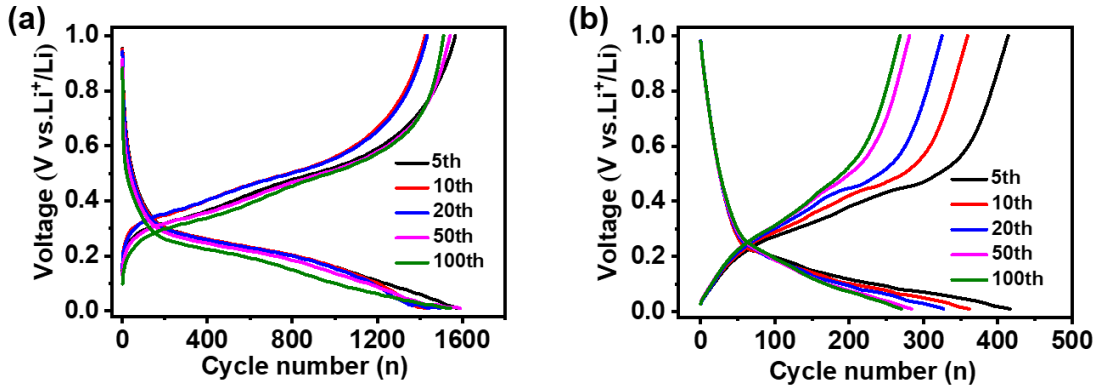

Figure S13. The voltage-capacity plots of the SiO_x/C composite with hydrothermal reaction for (a) 20 h and (b) 30 h.

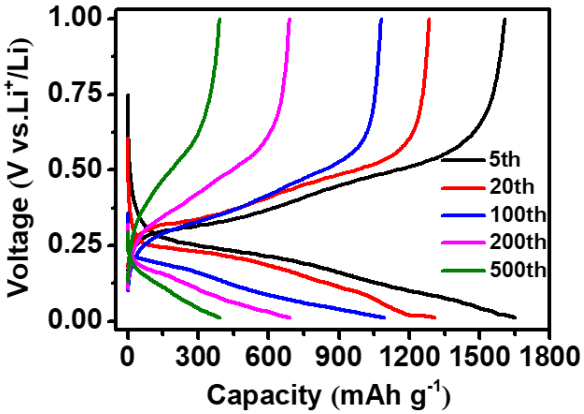

Figure S14. Galvanostatic voltage profiles of pristine Si electrode at different cycles.

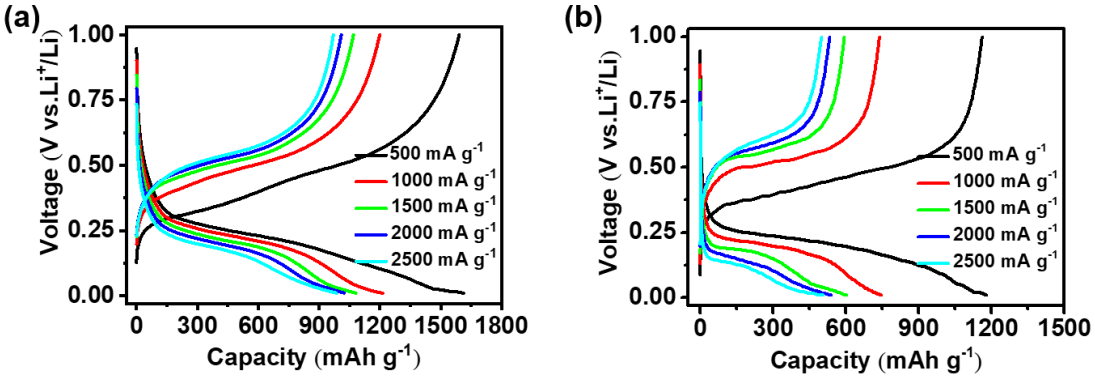

Figure S15. Galvanostatic voltage profiles at various current densities of (a) the SiO_x/C electrode, and (b) the pristine Si electrode.

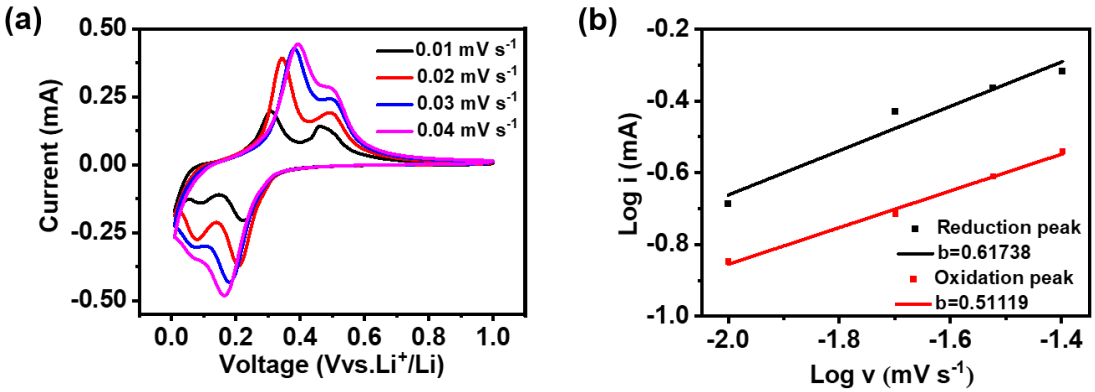

Figure S16. (a) CV curves of the pristine Si anode at different scan rates from 0.01 to 0.04 mV s^{-1}. (b) Determination of b-value through the fitted linear lines of log i and log v on redox peaks of pristine Si anode.

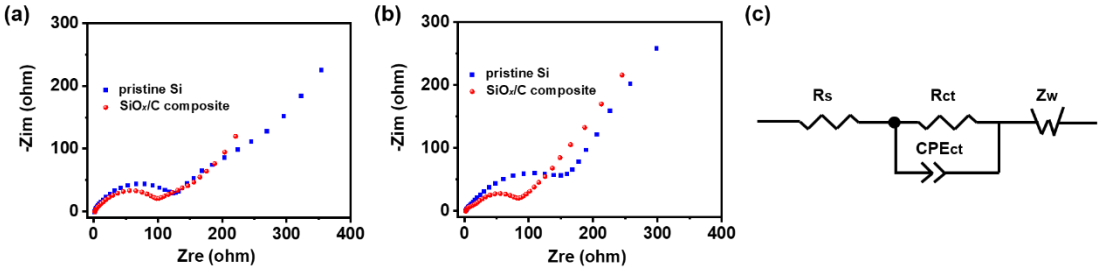

Figure S17. Electrochemical impedance spectra of the SiO_x/C composite and pristine Si electrodes after (a) the initial activation cycles and (b) 50 cycles, (c) the corresponding equivalent circuit model. R_s at high frequency represents resistance between the electrolyte and electrode. R_{ct} and CPE_{ct} are indicators of the charge transfer resistance and constant phase element. Z_w is assigned to the Warburg diffusion process of Li^+ through electrodes.

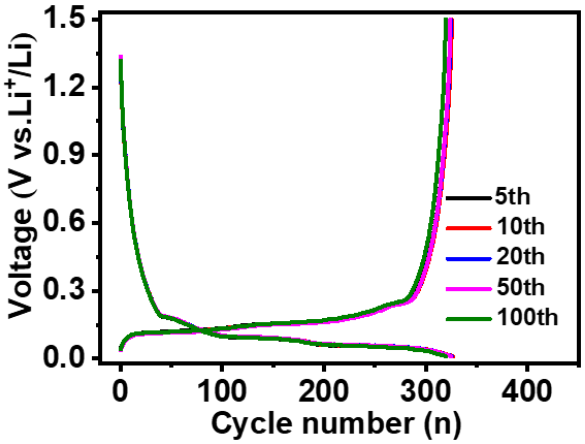

Figure S18. Galvanostatic voltage profiles of graphite electrode at different cycles.